

COMPUTER ASSISTED PROOFS OF TWO-DIMENSIONAL ATTRACTING INVARIANT TORI FOR ODES

MACIEJ J. CAPIŃSKI*

AGH University of Science and Technology
al. Mickiewicza 30, 30-059 Kraków, Poland

EMMANUEL FLEURANTIN AND J.D. MIRELES JAMES

Florida Atlantic University
777 Glades Rd., Boca Raton, FL 33431, USA

(Communicated by the associate editor name)

ABSTRACT. This work studies existence and regularity questions for attracting invariant tori in three dimensional dissipative systems of ordinary differential equations. Our main result is a constructive method of computer assisted proof which applies to explicit problems in non-perturbative regimes. We obtain verifiable lower bounds on the regularity of the attractor in terms of the ratio of the expansion rate on the torus with the contraction rate near the torus. We consider separately two important cases of rotational and resonant tori. In the rotational case we obtain C^k lower bounds on the regularity of the embedding. In the resonant case we verify the existence of tori which are only C^0 and neither star-shaped nor Lipschitz.

1. Introduction. Questions about the existence, topology, and regularity of invariant sets have organized the qualitative theory of nonlinear dynamics since the foundational work of Poincaré at the end of the Nineteenth Century. In modern times numerical simulations play a crucial role in this theory, providing deeper insights into the fine structure of phase space than can be obtained by any other means. The digital computer has emerged as a kind of dynamical systems laboratory, where one runs experiments on nonlinear systems far from a trivial solution or other perturbative regime.

In response to this development last four decades have seen a number of researchers put tremendous energy into developing and deploying computer assisted methods of proof which bridge the gap between numerical conjecture and mathematically rigorous theorems. The work of Lanford, Eckman, and Collet on the computer assisted proof of the Feigenbaum Conjectures [1, 2], and the resolution of Smale's 14th problem by Tucker [3, 4] provide excellent examples of this trend. The

2010 *Mathematics Subject Classification.* 34C45, 70K43, 37G35, 65P20, 65G20 .

Key words and phrases. Attracting invariant tori, computer assisted proof, dynamics of ordinary differential equations.

The first author is supported by the NCN grant 2018/29/B/ST1/00109 and by the Faculty of Applied Mathematics AGH UST statutory tasks 11.11.420.004 within subsidy of Ministry of Science and Higher Education. The work has been conducted during the visit to FAU sponsored by the Fulbright Foundation. The third author was partially supported by National Science Foundation grant DMS 1813501.

* Corresponding author: maciej.capinski@agh.edu.pl .

recent review articles [5, 6] provide historical context and more complete discussion of the literature.

The present work focuses on computer assisted methods of proof for attracting invariant tori in dissipative vector fields. Invariant tori typically appear in systems where there are two or more competing natural frequencies. Two common mechanisms are periodic/quasi-periodic perturbations of a system with an attracting periodic orbit, and when a periodic orbit with complex conjugate Floquet multipliers loses stability – triggering a Neimark-Sacker bifurcation in a Poincaré section [7, 8]. Both situations are treated in the present work. Some classic references on dissipative dynamical systems having invariant tori are [9, 10, 11, 12, 13, 14, 15, 16, 17], and we refer also to the works of [18, 19, 20, 21, 22, 23] for a functional analytic approach to this topic. Of course the study of robust invariant manifolds, or *normally hyperbolic invariant manifolds* (NHIMs) goes back to the classic works of Fenichel [24], and of Hirsch, Pugh, and Shub [25, 26, 27]. See also the works of [28, 29, 30, 31, 32, 33] and the references therein for some numerical investigations of NHIMs.

Related techniques for computer assisted proof of invariant tori are found in the works of [34, 35, 36, 37, 38, 39], and the references therein. It should be remarked that the works just cited deal with analytic invariant KAM tori in symplectic/Hamiltonian systems, where the torus cannot be attracting and the dynamics on the torus are conjugate to a Diophantine irrational rotation. The present work deals with attracting invariant tori in dissipative systems. These objects are necessarily of lower regularity [40] – C^k sometimes with $0 \leq k < \infty$ – and computer assisted existence proofs require different strategies.

Our analysis is formulated in terms of topological and geometric hypotheses which we check using mathematically rigorous computational techniques for numerical integration of vector fields and their variational equations. To make the presentation as self contained as possible we focus on the case of 3D fields and include elementary proofs of our arguments. We implement our method in two illustrative examples. The first example is a periodic perturbation of a planar vector field where the unperturbed system has an attracting periodic orbit. Here we prove the existence of C^k invariant tori with rotational dynamics. The second example is an autonomous vector field where resonant invariant tori appear naturally after a Neimark-Sacker bifurcation.

The two situations require different analysis. In the rotational case we develop an *outer approximation* of the torus via coverings by polygons and cone conditions. The union of the polygons is eventually shown to contain a torus. In the case of the autonomous vector field, where the invariant torus appears in a Neimark-Sacker bifurcation, the tori we consider are resonant. This means that they can be decomposed into attracting and saddle periodic orbits, where the unstable manifold of the saddle is absorbed completely into a trapping neighborhood of the attracting orbit. In the resonant case we provide an *inner approximation*, in the sense that we build the torus out of invariant pieces whose union is shown to be the desired torus. In both the rotational and resonant cases we study the tori away from the perturbative case. We remark that, because our theoretical arguments are formulated for maps (in our case Poincaré maps), our implementations rely heavily on the *validated C^k integrators* developed over the last decade by Wilczak and Zgliczyński [41, 42].

A technical remark is that our analysis of the rotational tori is formulated for a star-shaped region in an appropriate surface of section. The star-shaped hypothesis is an implementation detail which allows us to proceed without making a technical digression into the setting of vector bundles. Nevertheless, we indicate in Section 3.3 how to proceed more generally. A second technical remark is that the torus may be smoother than we are actually able to prove. Put another way, we prove that the rotational torus is *at least* C^k though it may in fact be smoother. We do not claim that our regularity results are sharp. On the other hand the resonant tori we study are globally only C^0 , and in this case the regularity is sharp as the tori are not globally Lipschitz.

The remainder of the paper is organized as follows. In Section 2 we review some preliminary notions and definitions from dynamics and validated numerics. In Section 3 we state and prove our main theorem on the existence of attracting invariant Lipschitz curves, and investigate conditions which imply their differentiability.

Section 4 treats computer assisted methods of validation for the existence of homoclinic/heteroclinic orbits for planar maps. More explicitly we develop techniques for proving the existence of attracting fixed points and obtaining lower bounds on the size of the basin of attraction. Then we recall some tools for validating bounds on the local stable/unstable manifolds attached to saddle fixed points from [43, 44]. Finally we prove the existence of heteroclinic connections from the saddle to the attractor. When these techniques are applied in a Poincaré section for an ODE we obtain connections between periodic orbits of the differential equation.

In Section 5 we show how to apply the methods of Section 4 to prove the existence of invariant tori for ODEs. The main idea is to propagate an invariant circle from a Poincaré section by the flow of the ODE.

Section 6 is devoted to the implementation of our methods in two example applications. We consider a periodically forced Van der Pol equation where the natural attracting periodic orbit in the unforced system gives an attracting invariant torus after the application of the forcing. Here we prove the existence of C^k invariant tori. We also consider an autonomous differential equation with an attracting resonant tori. There is an attracting periodic orbit in the invariant torus which has complex conjugate multipliers, hence the torus is only C^0 .

2. Preliminaries. For a set A we write \bar{A} to denote its closure, $\text{int}A$ to denote its interior, and write \mathbb{S}^1 for a one dimensional circle. Throughout the paper, for $x \in \mathbb{R}^n$ we shall use $\|x\|$ to stand for the Euclidean norm. Let $B(p, r)$ denote the open ball of radius r centered at p .

Suppose that $f : \mathbb{R}^n \rightarrow \mathbb{R}^n$ is a diffeomorphism and let $p^* \in \mathbb{R}^n$ be a hyperbolic fixed point of f (i.e. the eigenvalues of $Df(p^*)$ are not on the unit circle). We shall use the notation $W^u(p^*)$ and $W^s(p^*)$ to stand for the unstable and the stable manifold of p^* , respectively, i.e.

$$\begin{aligned} W^u(p^*) &= \{p : \|f^n(p) - p^*\| \rightarrow 0 \text{ as } n \rightarrow -\infty\}, \\ W^s(p^*) &= \{p : \|f^n(p) - p^*\| \rightarrow 0 \text{ as } n \rightarrow \infty\}. \end{aligned}$$

For $f : \mathbb{R}^n \rightarrow \mathbb{R}^n$ and $B \subset \mathbb{R}^n$ define $[Df(B)] \subset \mathbb{R}^n \times \mathbb{R}^n$ as

$$[Df(B)] := \left\{ (a_{ij})_{i,j=1}^n : a_{ij} \in \left[\inf_{p \in B} \frac{\partial f_i}{\partial x_j}(p), \sup_{p \in B} \frac{\partial f_i}{\partial x_j}(p) \right] \text{ for } i, j = 1, \dots, n \right\}.$$

We refer to $[Df(B)]$ as the interval enclosure of the derivative of f on B , and write Id for the identity matrix.

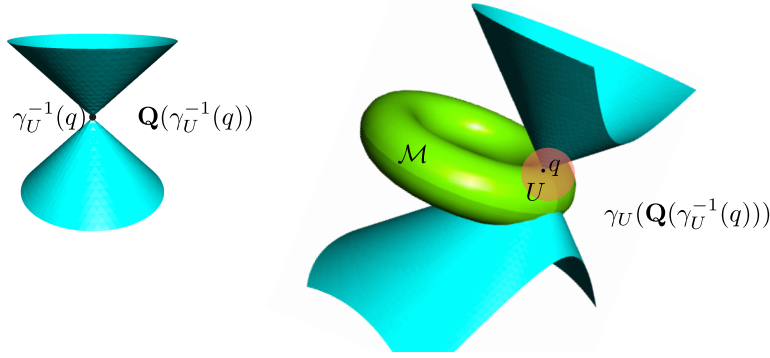


FIGURE 1. On the left we have a cone attached at the point $\gamma_U^{-1}(q)$ in the case when $k = 2$ and $n = 3$. Note that the cone is *not* the blue (cone shaped) set. The cone $\mathbf{Q}(\gamma_U^{-1}(q))$ is the complement of the blue set in \mathbb{R}^3 ; i.e. the white region outside of the blue set. On the right we have an example of a Lipschitz manifold.

For an interval matrix \mathbf{A} , i.e. a set $\mathbf{A} \subset \mathbb{R}^{n \times n}$, we will write

$$\|\mathbf{A}\| := \sup \{\|Ax\| : \|x\| = 1, A \in \mathbf{A}\}.$$

We say that \mathbf{A} is invertible if each $A \in \mathbf{A}$ is invertible. We define $\mathbf{A}^{-1} := \{A^{-1} : A \in \mathbf{A}\} \subset \mathbb{R}^n \times \mathbb{R}^n$.

The following lemma is a version of the mean value theorem, which is useful in a number of places throughout the paper.

Lemma 2.1. *Let $f : \mathbb{R}^n \rightarrow \mathbb{R}^n$ be C^1 , let $B \subset \mathbb{R}^n$ be a cartesian product of closed intervals in \mathbb{R}^n and let $p_1, p_2 \in B$, then we can choose an $n \times n$ matrix $A \in [Df(B)]$ for which we will have*

$$f(p_1) - f(p_2) = A(p_1 - p_2).$$

with

$$A = \int_0^1 Df(p_2 + t(p_1 - p_2)) dt.$$

We use the following classical result.

Theorem 2.2. [45] *(Interval Newton method) Let $f : \mathbb{R}^n \rightarrow \mathbb{R}^n$ be a C^1 function and B be a cartesian product of closed intervals in \mathbb{R}^n . If $[Df(B)]$ is invertible and there exists an x_0 in B such that*

$$N(x_0, B) := x_0 - [Df(B)]^{-1} f(x_0) \subset B,$$

then there exists a unique point $x^ \in B$ such that $f(x^*) = 0$.*

The notion of a Lipschitz manifold requires us to define certain cone conditions. Fix $1 \leq k \leq n$ and for a point $x = (x_1, \dots, x_n) \in \mathbb{R}^n$ write $\pi_{x_1, \dots, x_k}(x) := (x_1, \dots, x_k)$ and $\pi_{x_{k+1}, \dots, x_n}(x) = (x_{k+1}, \dots, x_n)$. For a point $p \in \mathbb{R}^n$ we define the cone attached to p as (see Figure 1)

$$\mathbf{Q}_k(p) := \{x \in \mathbb{R}^n : a \|\pi_{x_1, \dots, x_k}(p - x)\| \geq \|\pi_{x_{k+1}, \dots, x_n}(p - x)\|\},$$

where $0 < a \in \mathbb{R}$ is a fixed constant. We suppress the k subscript and simply write $\mathbf{Q}(p)$ when k is clear from context.

Definition 2.3. Let $\mathcal{M} \subset \mathbb{R}^n$ be a k -dimensional compact topological manifold. We say that $\mathcal{M} \subset \mathbb{R}^n$ is Lipschitz, if it satisfies cone conditions in the following sense: any point $p \in \mathcal{M}$ there exists an open neighborhood U of p in \mathbb{R}^n , an open set $B \subset \mathbb{R}^n$, and a C^1 diffeomorphism $\gamma_U : B \rightarrow U$ such that for any $q \in \mathcal{M} \cap U$ (see Figures 1, 2)

$$\mathcal{M} \cap U \subset \gamma_U \left(\mathbf{Q} \left(\gamma_U^{-1}(q) \right) \cap B \right).$$

3. Attracting invariant circles for maps on \mathbb{R}^2 . In this Section we discuss how to establish the existence of attracting invariant curves for planar maps. The methodology is based on taking a neighborhood of the curve and validating that this neighborhood maps into itself. This on its own ensures only existence of an invariant set, and not that the set is a curve. We therefore consider two additional conditions. The first is that we have a ‘well aligned cone field’ which also maps into itself, and the second is that we have uniform contraction inside of the considered set.

The proposed method is similar in spirit to [46, 47]. The main difference is that the papers just mentioned work with a vector bundle around the manifold. In the present work we formulate our results in local coordinates that roughly cover (see Figure 2) the investigated invariant curve, removing the need for vector bundle coordinates. This simplifies the implementation of the method.

We give our proof in the setting of closed star-shaped invariant curves. Our results can be directly generalized to the setting where we have a vector bundle based on a closed curve (not necessarily star-shaped) in \mathbb{R}^2 . We present this generalization in Section 3.3. We give our proofs in the star-shaped setting due to the simplicity of the setup. The arguments for the more general case of vector bundles are analogous.

In Section 3.1 we present the method which ensures the existence of Lipschitz invariant curves, in Section 3.2 we add conditions which ensure the C^k smoothness, and in Section 3.4 we discuss how the assumptions are validated in practice.

3.1. Establishing closed attracting star-shaped curves. Let

$$f : \mathbb{R}^2 \rightarrow \mathbb{R}^2$$

be a C^1 diffeomorphism¹. Assume that $B_1, B_2 \subset \mathbb{R}^2$ are homeomorphic to two dimensional open balls in \mathbb{R}^2 and that $\overline{B_1} \subset B_2$. Let $U := \overline{B_2} \setminus B_1$ and assume that

$$U = \bigcup_{i=1}^N U_i = \bigcup_{i=1}^N \gamma_i(M_i), \quad (1)$$

where for each $i = 1, \dots, N$, the $M_i = [-R_i, R_i] \times [-r_i, r_i]$ for some fixed sequence of constants $0 < r_i, R_i \in \mathbb{R}$, and $\gamma_i : M_i \rightarrow \mathbb{R}^2$ are diffeomorphisms onto their image (See Figure 2). We think of γ_i as local coordinates on the set U .

Our objective is to provide conditions ensuring the existence of a star-shaped Lipschitz closed curve in U homeomorphic to a circle and invariant under f .

¹For the purposes of this Section we could assume that f is a homeomorphism, however the validation of the required assumptions is easier using the derivative of f . This is why we assume C^1 smoothness straightaway.

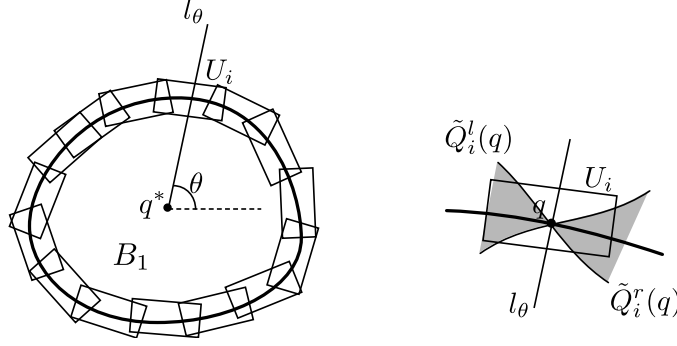


FIGURE 2. The set U is a collection of boxes, and we prove the existence of a star-shaped invariant closed curve around q^* which satisfies the cone conditions.

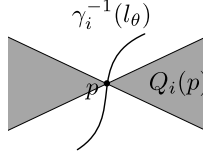


FIGURE 3. A well aligned cone.

We equip each box M_i with cones as follows. For $p \in \mathbb{R}^2$ define

$$\begin{aligned} Q_i(p) &= \{(x, y) : |y - \pi_y p| \leq a_i |x - \pi_x p|\}, \\ Q_i^r(p) &= Q_i(p) \cap \{(x, y) : x > \pi_x p\}, \\ Q_i^l(p) &= Q_i(p) \cap \{(x, y) : x < \pi_x p\}, \end{aligned} \quad (2)$$

where $0 < a_1, \dots, a_N \in \mathbb{R}$ are fixed constants. The superscripts r and l stand for ‘right’ and ‘left’, respectively. Define (see Figure 2)

$$\begin{aligned} \tilde{Q}_i(q) &:= \gamma_i(Q_i(\gamma_i^{-1}(q))), \\ \tilde{Q}_i^\kappa(q) &:= \gamma_i(Q_i^\kappa(\gamma_i^{-1}(q))), \quad \text{for } \kappa \in \{r, l\}, \end{aligned}$$

and choose $q^* \in B_1 \subset \mathbb{R}^2$. (From now on the q^* will remain fixed.) We define the half line emanating from q^* at an angle θ as

$$l_\theta := \{p \in \mathbb{R}^2 : p = q^* + t(\cos \theta, \sin \theta) \text{ for } t > 0\}.$$

Definition 3.1. We say that the cones Q_i are well aligned if for any $\theta \in [0, 2\pi)$, $i \in \{1, \dots, N\}$ and $p \in \gamma_i^{-1}(U_i \cap l_\theta)$ we have

$$Q_i(p) \cap \gamma_i^{-1}(l_\theta) = p,$$

and $\gamma_i^{-1}(l_\theta)$ intersects $\{y - \pi_y p = a_i(x - \pi_x p)\}$ and $\{y - \pi_y p = -a_i(x - \pi_x p)\}$ transversally. (See Figure 3.)

Definition 3.2. Let $h : \mathbb{S}^1 \rightarrow \mathbb{R}^2$ be a continuous function. We say that h is a star-shaped closed curve around q^* if

$$h(\mathbb{S}^1) \cap l_\theta = h(\theta),$$

for all $\theta \in \mathbb{S}^1$.

Definition 3.3. We say that $h : \mathbb{S}^1 \rightarrow \mathbb{R}^2$ is a star-shaped closed curve which satisfies cone conditions, if it is a closed curve around q^* , and for any θ there exists an $i \in \{1, \dots, N\}$ and $r > 0$ such that (see Figure 2)

$$h(\mathbb{S}^1) \cap B(h(\theta), r) \subset \tilde{Q}_i(h(\theta)). \quad (3)$$

Definition 3.4. We say that f satisfies cone conditions if for any $i \in \{1, \dots, N\}$ and any $p \in \text{int}U_i$ there exists an $r > 0$ and $j \in \{1, \dots, N\}$ such that

$$f(\tilde{Q}_i^r(p) \cap B(p, r)) \subset \tilde{Q}_j^r(f(p)) \quad \text{and} \quad f(\tilde{Q}_i^l(p) \cap B(p, r)) \subset \tilde{Q}_j^l(f(p)) \quad (4)$$

or

$$f(\tilde{Q}_i^l(p) \cap B(p, r)) \subset \tilde{Q}_j^r(f(p)) \quad \text{and} \quad f(\tilde{Q}_i^r(p) \cap B(p, r)) \subset \tilde{Q}_j^l(f(p)). \quad (5)$$

Definition 3.5. Let μ be the Lebesgue measure on \mathbb{R}^2 . We shall say that f is uniformly attracting on U , if there exists a constant $0 \leq \lambda < 1$ such that for any Borel set $A \subset U$ we have $\mu(f(A)) \leq \lambda\mu(A)$.

We now formulate our main result with which we establish the existence of attracting invariant curves.

Theorem 3.6. *Assume that the cones Q_i are well aligned. Assume also that there exists a sequence of points in U , such that the piecewise affine circle which results from joining these points is a closed curve which satisfies cone conditions around q^* . If f is uniformly contracting on U , and if f satisfies cone conditions, and if $f(U) \subset \text{int}U$, then there exists a closed curve h^* around q^* , which satisfies cone conditions, such that $f(h^*) = h^*$. Moreover, for any $p \in U$, the orbit $\{f^n(p)\}_{n=0}^\infty$ accumulates on the curve h^* . That is, the ω -limit set of the orbit is contained in h^* .*

Proof. The proof is based on the following graph transform type argument. Let h be a closed curve around q^* , which satisfies cone conditions. We show that $f(h(\mathbb{S}^1))$ is the image of another closed curve around q^* , which satisfies cone conditions. Then we show iterates of h converge to h^* . Below we provide the details.

Since f is a homeomorphism $f(h(\mathbb{S}^1))$ is a circle. We claim that

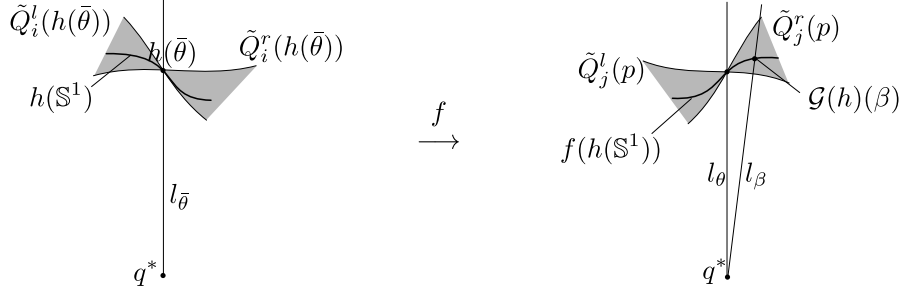
$$f(h(\mathbb{S}^1)) \cap l_\theta \neq \emptyset \quad \text{for any } \theta \in \mathbb{S}^1. \quad (6)$$

To see this, let $g : \mathbb{S}^1 \rightarrow \mathbb{R}$ be defined as

$$g(\theta) = \begin{cases} 1 & \text{if } f(h(\mathbb{S}^1)) \cap l_\theta \neq \emptyset, \\ 0 & \text{otherwise.} \end{cases}$$

Once we show that g is continuous, this will prove (6). This is because from $f(h(\mathbb{S}^1)) \subset f(U) \subset U$ and $U \cap q^* = \emptyset$ it follows that $q^* \notin f(h(\mathbb{S}^1))$ so for at least one $\theta \in \mathbb{S}^1$ we must have $g(\theta) = 1$; then, by continuity, we will have $g \equiv 1$. Since $g \equiv 1$, this circle intersects l_θ for every $\theta \in \mathbb{S}^1$, which implies (6).

To establish the continuity we start by showing that if $g(\theta) = 0$, then for β sufficiently close to θ we will have $g(\beta) = 0$. Suppose that $g(\theta) = 0$. Since $f(h(\mathbb{S}^1)) \subset f(U) \subset U$ we see that $f(h(\mathbb{S}^1))$ and $l_\theta \cap U$ are disjoint compact sets. This means that we can find their open neighborhoods, which will also be disjoint. Therefore $f(h(\mathbb{S}^1)) \cap l_\beta = \emptyset$ for β close to θ , hence $g(\beta) = 0$, as required.

FIGURE 4. Construction of $\mathcal{G}(h)$.

We now show that if $g(\theta) = 1$, then for β sufficiently close to θ we will have $g(\beta) = 1$. Let $p \in f(h(\mathbb{S}^1)) \cap l_{\theta}$. There exists a $\bar{\theta}$ such that $p = f(h(\bar{\theta}))$. Take i such that $h(\bar{\theta}) \in U_i$. From (3), for $\bar{\beta}$ close to $\bar{\theta}$

$$h(\bar{\beta}) \in \tilde{Q}_i(h(\bar{\theta})).$$

Since h is a closed curve around q^* we see that we have either

$$\bar{\beta} < \bar{\theta} \implies h(\bar{\beta}) \in \tilde{Q}_i^l(h(\bar{\theta})) \quad \text{and} \quad \bar{\beta} > \bar{\theta} \implies h(\bar{\beta}) \in \tilde{Q}_i^r(h(\bar{\theta})), \quad (7)$$

or

$$\bar{\beta} < \bar{\theta} \implies h(\bar{\beta}) \in \tilde{Q}_i^r(h(\bar{\theta})) \quad \text{and} \quad \bar{\beta} > \bar{\theta} \implies h(\bar{\beta}) \in \tilde{Q}_i^l(h(\bar{\theta})). \quad (8)$$

Without loss of generality let us assume that we have (7). (If we have (8) then the proof follows from mirror arguments.) We know that f satisfies cone conditions. Let us therefore assume that we have (4), from which it follows that for some j

$$f(h(\bar{\beta})) \in \tilde{Q}_j^r(f(h(\bar{\theta}))) = \tilde{Q}_j^r(p) \quad \text{for } \bar{\beta} > \bar{\theta}, \quad (9)$$

$$f(h(\bar{\beta})) \in \tilde{Q}_j^l(f(h(\bar{\theta}))) = \tilde{Q}_j^l(p) \quad \text{for } \bar{\beta} < \bar{\theta}. \quad (10)$$

(If we have (5) then the proof will follow from mirror arguments.) For any β sufficiently close to θ there will therefore exist a $\bar{\beta}$ such that $f(h(\bar{\beta})) \in l_{\beta}$; see Figure 4. Since $f(h(\bar{\beta})) \in f(h(\mathbb{S}^1))$ we see that for β sufficiently close $g(\beta) = 1$, as required.

We have established (6). We will now define a function $\mathcal{G}(h) : \mathbb{S}^1 \rightarrow U$, which we will prove to be a closed curve around q^* which has the same graph as $f(h(\mathbb{S}^1))$. (We use the notation $\mathcal{G}(h)$ since the function follows from a “graph transform” type construction.) We start by taking $\theta = 0$ and defining $\mathcal{G}(h)(0)$ to be any point from $f(h(\mathbb{S}^1)) \cap l_{\theta}$. At this stage we do not know if such point is unique, so we choose an arbitrary point from the intersection. Take j_0 such that $\mathcal{G}(h)(0) \in U_{j_0}$. From (9–10) we see that for $\theta > 0$ close to zero, we can extend $\mathcal{G}(h)$ to obtain a curve by defining $\mathcal{G}(h)(\theta) = f(h(\mathbb{S}^1)) \cap l_{\theta} \cap \tilde{Q}_{j_0}(\mathcal{G}(h)(0))$, as long as $\mathcal{G}(h)(\theta)$ remains in U_{j_0} . Let $\theta_1 > 0$ be some angle such that $\mathcal{G}(h)(\theta_1) \in U_{j_0} \cap U_{j_1}$, for some index j_1 . We can then continue our construction for $\theta > \theta_1$ as $\mathcal{G}(h)(\theta) = f(h(\mathbb{S}^1)) \cap l_{\theta} \cap \tilde{Q}_{j_1}(\mathcal{G}(h)(\theta_1))$. Continuing in this manner, we can reach $\theta = 2\pi$. We are sure that at $\theta = 2\pi$ we return to $\mathcal{G}(h)(0)$, since if this were not the case then we could continue with the construction and $f(h(\mathbb{S}^1))$ would contain an infinite spiral. This is not possible since $f(h(\mathbb{S}^1))$ is homeomorphic to a circle. From (9–10) we see that $\mathcal{G}(h)$ satisfies cone conditions, which also implies that it is continuous.

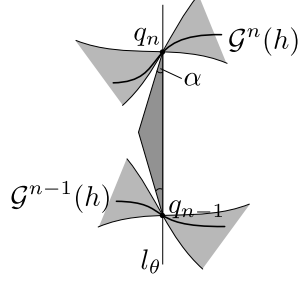


FIGURE 5. Since $\mathcal{G}^n(h)$ and $\mathcal{G}^{n-1}(h)$ satisfy cone conditions, we can find an angle α , such that the isosceles triangle, with base joining q_n and q_{n-1} , as in above plot, will fit between $\mathcal{G}^n(h)$ and $\mathcal{G}^{n-1}(h)$. By compactness of U and the fact that we have a finite number of C^1 local maps γ_i , the α can be chosen independently of n, θ, q_n and of q_{n-1} . This means that the area between $\mathcal{G}^n(h)$ and $\mathcal{G}^{n-1}(h)$ is bounded from below by $C\|q_n - q_{n-1}\|^2$, where $C > 0$ is some constant independent from n and θ .

We now show that by starting with the closed curve h which connects the points from the assumption of the theorem, then as we iterate the above defined graph transform we shall converge to the curve we seek; i.e.

$$\lim_{n \rightarrow \infty} \mathcal{G}^n(h) = h^*.$$

Convergence follows from the assumption that f is uniformly contracting on U .

For $n = 1, 2, \dots$ let A_n be the area between the curves $\mathcal{G}^n(h)$ and $\mathcal{G}^{n-1}(h)$. Since f is uniformly contracting, $A_n \leq \lambda^{n-1} A_1$. Let us consider two points, $q_n \in \mathcal{G}^n(h) \cap l_\theta$ and $q_{n-1} \in \mathcal{G}^{n-1}(h) \cap l_\theta$, for some $\theta \in \mathbb{S}^1$. Since the curves $\mathcal{G}^n(h)$ and $\mathcal{G}^{n-1}(h)$ satisfy cone conditions the area between them has to be at least $C\|q_n - q_{n-1}\|^2$, where $C > 0$ is a constant independent of the choice of θ and n . See Figure 5 and the caption below it. This gives us

$$C\|q_n - q_{n-1}\|^2 \leq A_n \leq \lambda^{n-1} A_1$$

so

$$\|q_n - q_{n-1}\| \leq (\sqrt{\lambda})^{n-1} \sqrt{\frac{A_1}{C}},$$

from which, by the fact that $\sqrt{\lambda} < 1$, it follows that the sequence q_n is convergent. This means that we can define $h^*(\theta) := \lim_{n \rightarrow \infty} \mathcal{G}^n(h)(\theta)$. All $\mathcal{G}^n(h)$ are closed curves around q^* , which satisfy cone conditions. This property is preserved when passing to the limit, which concludes the proof. \square

3.2. Smoothness. In this Section we discuss how to establish that the invariant curve h^* from Theorem 3.6 is smooth. We first need to introduce some notation.

Consider local maps $f_{ji} : [-R_i, R_i] \times [-r_i, r_i] \supset \text{domain } f_{ji} \rightarrow \mathbb{R}^2$ defined as

$$f_{ji} := \gamma_j^{-1} \circ f \circ \gamma_i.$$

(The domain of f_{ji} can be empty.) We now define the following constants

$$\begin{aligned}\xi &:= \inf \left\{ \left| \frac{\partial (\pi_x f_{ji})}{\partial x}(q) - a_j \right| \left| \frac{\partial (\pi_x f_{ji})}{\partial y}(q) \right| : i, j = 1, \dots, N, q \in \text{domain} f_{ij} \right\}, \\ \mu &:= \sup \left\{ \left| \frac{\partial (\pi_y f_{ji})}{\partial y}(q) \right| + a_j \left| \frac{\partial (\pi_x f_{ji})}{\partial y}(q) \right| : i, j = 1, \dots, N, q \in \text{domain} f_{ij} \right\}.\end{aligned}$$

Definition 3.7. We say that f satisfies rate conditions of order k if $\xi > 0$ and for any $j \in \{1, \dots, k\}$

$$\frac{\mu}{\xi^{j+1}} < 1. \quad (11)$$

Remark 1. The definition is a simplified version of the rate condition considered in [47]. There are two differences. The first is that in [47] three coordinates are considered: the unstable, the stable and central coordinate. Here we only have two: the central coordinate x and the stable coordinate y . The second difference is that the rate conditions considered in [47] include also bounds needed to establish the existence of the invariant manifold. Here we do this using the slightly modified method from Theorem 3.6. Because of these two differences, the nine inequalities for rate conditions from [47] are reduced to the single inequality (11). (The condition (11) corresponds to the first inequality in equation (4) from [47].)

Below theorem is a reformulation of the smoothness result from [47], adapted to our simplified setting.

Theorem 3.8. *If in addition to all assumptions of Theorem 3.6 the map f satisfies rate conditions of order k , then h^* established in Theorem 3.6 is C^k .*

Proof. The result follows from Lemma 48 in [47]. In our setting the only needed condition to apply Lemma 48 from [47] is the condition (11); see the remark in the third bullet list item on page 6226 in [47]. Lemma 48 from [47] ensures that when we iterate the graph transform from the proof of Theorem 3.6 starting with a C^k curve h^0 , then the C^k smoothness persists as we pass to the limit. In the proof of Theorem 3.6 we take h^0 to be a piecewise affine circle. We can smooth out the corners of such curve to make it C^k , so the fact that the smoothness is preserved in the limit ensures the claim. \square

3.3. Generalization to the setting of vector bundles. In this section we present how the results from Sections 3.1 and 3.2 can be generalized. Let us consider a closed curve $p^* \subset \mathbb{R}^2$, parameterized by $\theta \in \mathbb{S}^1$, i.e. $p^* : \mathbb{S}^1 \rightarrow \mathbb{R}^2$. Consider a vector bundle E in \mathbb{R}^2 with $p^*(\mathbb{S}^1)$ as its base and with fibers E_θ at $p^*(\theta)$, for $\theta \in \mathbb{S}^1$. Assume that the set $U \subset \mathbb{R}^2$ of the form (1) is a subset of E (see Figure 6). We will say that the family of cones Q_i introduced in the Section 3.1 is well aligned with E_θ , if it satisfies the assumptions of Definition 3.1, with l_θ changed to E_θ . We will say that $h : \mathbb{S}^1 \rightarrow \mathbb{R}^2$ is a closed curve around p^* iff $h(\mathbb{S}^1) \cap E_\theta = h(\theta)$ for all $\theta \in \mathbb{S}^1$. With such modifications Theorems 3.6 and 3.8 remain true. Their proofs in this more general setting are identical, with the only difference that l_θ needs to be changed to E_θ and q^* needs to be changed to p^* throughout the arguments.

The main difficulty in this setting is actually constructing the needed vector bundles in particular examples, and this is the technicality overcome using the star-shaped assumption in our earlier arguments. The interested reader is referred to [46, 47] for more general discussion.

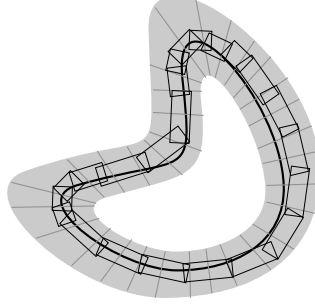


FIGURE 6. Generalization to a vector bundle setting. The vector bundle E is in grey, its base is the curve p^* , which is in black, with the fibers E_θ represented as the grey lines. The set U consists of the union of the small rectangles. Note that in this picture p^* is not the invariant curve, rather it is the base of the vector bundle.

3.4. Validation of assumptions. We finish this Section by describing how the assumptions of Theorems 3.6, 3.8 are validated in practice. For the applications we have in mind we take γ_i to be affine maps, so checking that Q_i are well aligned is a simple linear algebra exercise of checking that $Q_i(p)$ and $\gamma_i^{-1}(l_\theta)$ intersect at one and only one point. For instance, when $\gamma_i(q) = A_i q + q_i$ (with a matrix A_i and point $q_i \in \mathbb{R}^2$) one checks that for any θ such that $U_i \cap l_\theta \neq \emptyset$ for $v_\theta = A_i^{-1}((\cos \theta, \sin \theta))$ we have $|\pi_y v_\theta| > a_i |\pi_x v_\theta|$. This condition is checked with computer assistance.

Next we take a sequence of points q_1, \dots, q_N around q^* (in our application we take the points q_i to be the same as those used to define the affine maps γ_i) and validate that lines joining q_i with q_{i+1} (and the line joining q_N with q_1) lie inside the cones $\tilde{Q}_i(q_i)$ and $\tilde{Q}_{i+1}(q_{i+1})$, respectively (and the cones $\tilde{Q}_N(q_N)$ and $\tilde{Q}_1(q_1)$, respectively). This is also done with computer assistance.

To check that f is uniformly contracting in U we check that for any $i \in \{1, \dots, N\}$ and any matrix $A \in [Df(U_i)]$ we have $|\det(A)| < 1$. This is particularly simple to do in our case, as the computation of determinants of 2×2 matrices is straightforward. Once again, this is done with computer assistance.

The condition that $f(U)$ is a subset of U can be done directly by taking $U_i = \bigcup_{k=1}^m U_{i,k}$ for some chosen $U_{i,k}$ and checking that for any $i \in \{1, \dots, N\}$ and $k \in \{1, \dots, m\}$ there exists a $j \in \{1, \dots, N\}$ such that $f(U_{i,k}) \subset U_j$. In our computer assisted approach we do this by taking

$$M_{i,k} := \left[-R_i + (k-1)\frac{2R_i}{m}, -R_i + k\frac{2R_i}{m} \right] \times [-r_i, r_i],$$

$U_{i,k} := \gamma_i(M_{i,k})$ and checking that for some $j \in \{1, \dots, N\}$

$$\gamma_j^{-1} \circ f \circ \gamma_i(M_{i,k}) \subset M_j. \quad (12)$$

The computation just described, which is done in the “local coordinates”, is well suited to interval arithmetic implementation provided the maps γ_i are well aligned with the invariant curve we wish to established. When γ_l are affine maps, i.e. $\gamma_l(q) = A_l q + q_l$ condition (12) is validated by using Lemma 2.1 by taking a point $v_{i,k} \in M_{i,k}$ and checking that

$$\gamma_j^{-1} \circ f \circ \gamma_i(M_{i,k}) \subset \gamma_j^{-1} \circ f \circ \gamma_i(v_{i,k}) + (A_j^{-1}[Df(\gamma_i(M_{i,k}))] A_i)(M_{i,k} - v_{i,k}). \quad (13)$$

With a good choice of the matrices A_l the matrix $A_j^{-1} [Df(\gamma_i(M_{i,k}))] A_i$ can be made close to diagonal, which helps to reduce the wrapping effect of interval arithmetic computations. In this case the derivatives of the local maps are bounded by

$$Df_{ji}(q) \in A_j^{-1} [Df(\gamma_i(M_{i,k}))] A_i \quad \text{for } q \in M_{i,k}, \quad (14)$$

and these can be used to compute the coefficients μ, ξ needed for the rate conditions.

The next lemma is used to validate cone conditions. We express it in a more general setting where the map is defined on \mathbb{R}^n , as this setting is needed in Section 4. Below we state the result using the notations f and M , but for our purposes here one would apply it for a local map f_{ji} on a set $M_{i,k}$, with the bound on the derivative from (14). (We remove the subscripts to simplify the statement and to make it more compatible with the story from Section 4.)

Lemma 3.9. *Let $f : \mathbb{R} \times \mathbb{R}^{n-1} \rightarrow \mathbb{R} \times \mathbb{R}^{n-1}$ and let $M \subset \mathbb{R}^n$. Let $a_1, a_2 > 0$ and*

$$\begin{aligned} Q_1(p) &= \{(x, y) \in \mathbb{R} \times \mathbb{R}^{n-1} : a_1 |x - \pi_x p| \geq \|y - \pi_y p\|\}, \\ Q_2(p) &= \{(x, y) \in \mathbb{R} \times \mathbb{R}^{n-1} : a_2 |x - \pi_x p| \geq \|y - \pi_y p\|\}. \end{aligned}$$

If for any $v = (1, v_y) \in Q_1(0)$ and any $A \in [Df(M)]$ we have $Av \in Q_2(0)$ then for any $p_1, p_2 \in M$ such that $p_2 \in Q_1(p_1)$ we have $f(p_2) \in Q_2(f(p_1))$.

Proof. If $p_1 = p_2$ the result is automatic. Assume that $p_1 \neq p_2$. Since $p_2 \in Q_1(p_1)$ we see that $\pi_x(p_1 - p_2) \neq 0$. By Lemma 2.1 for some $A \in [Df(B)]$ we have $f(p_1) - f(p_2) = A(p_1 - p_2)$. Take $v = \frac{p_1 - p_2}{|\pi_x(p_1 - p_2)|}$. Then since $Av \in Q_2(0)$ we have $\|\pi_y Av\| \leq a_2 |\pi_x Av|$ so in turn

$$\begin{aligned} \|\pi_y(f(p_1) - f(p_2))\| &= |\pi_x(p_1 - p_2)| \|\pi_y Av\| \\ &\leq |\pi_x(p_1 - p_2)| a_2 |\pi_x Av| \\ &= a_2 |\pi_x(f(p_1) - f(p_2))|, \end{aligned}$$

as required. \square

4. Heteroclinic connections between fixed points of maps. In this Section we discuss how to prove the existence of heteroclinic orbits between two fixed points of a map. We are interested in the case when one of the fixed points is hyperbolic, and the other fixed point is a stable focus. The heteroclinic orbits will be found in three steps. The first is to establish an attracting neighborhood for which all trajectories converge to the stable focus. This is discussed in Section 4.1. The second step is to establish a bound on the unstable manifold of the hyperbolic fixed point. This is described in Section 4.2. Lastly we propagate the unstable manifold by our map. If it reaches the attracting neighborhood of the stable focus then we have established a heteroclinic orbit. This is discussed in Section 4.3.

4.1. Establishing attracting fixed points. In this Section we show how one can obtain the existence of an attracting fixed point within a prescribed neighborhood. We start with a technical lemma.

Lemma 4.1. *Let $f : \mathbb{R}^n \rightarrow \mathbb{R}^n$ be C^1 , and $\lambda > 0$ be a fixed constant. Let B be a cartesian product of closed intervals in \mathbb{R}^n (an n -dimensional cube). If for any $A \in [Df(B)]$ the matrix $\lambda Id - A^\top A$ is strictly positive definite, then for any $p_1, p_2 \in B$*

$$\|f(p_1) - f(p_2)\|^2 < \lambda \|p_1 - p_2\|^2.$$

Proof. By Lemma 2.1 we can choose an $A \in [Df(B)]$ such that $f(p_1) - f(p_2) = A(p_1 - p_2)$. (The choice of A depends on p_1 and p_2 .) We therefore have

$$\begin{aligned} & \lambda \|p_1 - p_2\|^2 - \|f(p_1) - f(p_2)\|^2 \\ &= \lambda (p_1 - p_2)^\top (p_1 - p_2) - (f(p_1) - f(p_2))^\top (f(p_1) - f(p_2)) \\ &= \lambda (p_1 - p_2)^\top (p_1 - p_2) - (p_1 - p_2)^\top A^\top A (p_1 - p_2) \\ &= (p_1 - p_2)^\top (\lambda Id - A^\top A) (p_1 - p_2) \\ &> 0, \end{aligned}$$

where the last line follows from the fact that $\lambda Id - A^\top A$ is strictly positive definite. \square

Remark 2. To check that a matrix 2×2 matrix C is strictly positive definite, it is enough to establish that

$$\det(C) > 0 \quad \text{and} \quad \text{trace}(C) > 0.$$

The next lemma establishes that we have an attracting fixed point within a prescribed neighborhood.

Lemma 4.2. *Let $f : \mathbb{R}^n \rightarrow \mathbb{R}^n$ be C^1 . Let $\lambda \in (0, 1)$ be a fixed constant. Let B be a cartesian product of closed intervals in \mathbb{R}^n (an n -dimensional cube). If $f(B) \subset B$ and for any $A \in [Df(B)]$ the matrix $\lambda Id - A^\top A$ is strictly positive definite, then there exists an attracting fixed point of f in B . (By “attracting” we mean that for any $p \in B$, $f^k(p)$ will converge to the fixed point as k tends to infinity.)*

Proof. Since $\lambda \in (0, 1)$, by Lemma 4.1 we see that f is contracting, so the result follows from the Banach fixed point theorem. \square

4.2. Establishing unstable manifolds of hyperbolic fixed points. We now give a method for establishing mathematically rigorous bounds for a local unstable manifold of a hyperbolic fixed point. We restrict to the case where the unstable manifold is of dimension 1 as this is the case seen in the applications. Our method is based on [43], and a more general procedure is found in [44].

Let p^* be a hyperbolic fixed point of a C^1 map $f : \mathbb{R}^n \rightarrow \mathbb{R}^n$. Assume that the unstable eigenspace of p^* is of dimension $u = 1$. Assume that the unstable eigenvalue of $Df(p^*)$ is λ , with $|\lambda| > 1$.

Let B_u be a closed interval and let B_s be an $s := n - u = n - 1$ dimensional product of closed intervals (a closed cube in \mathbb{R}^s). Let $B = B_u \times B_s$ and assume that $p^* \in \text{int} B$. For any point $p \in \mathbb{R}^n = \mathbb{R}^u \times \mathbb{R}^s$ we shall write $p = (p_u, p_s)$. The subscripts u and s stand of “unstable” and “stable”, respectively. This notation is chosen since in our approach these coordinates will be roughly aligned with the unstable/stable eigenspaces of p^* . We will use the notation $\pi_u p = p_u$ and $\pi_s p = p_s$ for the projections.

Let $L > 0$ be a fixed constant. For any $p = (p_u, p_s) \in \mathbb{R}^u \times \mathbb{R}^s$ we define a cone centered at p as

$$Q(p) := \{q = (q_u, q_s) : \|q_s - p_s\| \leq L |q_u - p_u|\}. \quad (15)$$

Definition 4.3. We say that $h : B_u \rightarrow B_u \times B_s$ is a horizontal disc in B if it is continuous, if for any $x \in B_u$, $\pi_u h(x) = x$ and if $h(B_u) \subset Q(h(x))$.

In other words, horizontal discs are one dimensional curves in $B_u \times B_s$, which are graphs of Lipschitz functions with the Lipschitz constant L .

The next lemma is our main tool for establishing bounds on the unstable manifold of p^* .

Lemma 4.4. [43] *Assume that for any $p_1, p_2 \in B$ such that $p_2 \in Q(p_1)$ we have*

$$f(p_2) \in Q(f(p_1)). \quad (16)$$

Let $m \in (1, |\lambda|)$ be a fixed number. Assume that for any $p \in (Q(p^) \cap B) \setminus \{p^*\}$ we have*

$$\|f(p) - p^*\| > m \|p - p^*\|. \quad (17)$$

Then the unstable manifold of p^ is contained in $Q(p^*)$. Moreover, there exists a horizontal disc $w^u : B_u \rightarrow B$ in B such that the unstable manifold of p^* is the graph of w^u .*

We now discuss validation of the assumptions (16), (17) of Lemma 4.4. To verify (16) we use Lemma 3.9 (taking $M = B$ and $a_1 = a_2 = L$). To verify (17) we use the following lemma.

Lemma 4.5. [43] *Assume that*

$$[Df(B)] = \begin{pmatrix} \mathbf{A} & \mathbf{C}_{12} \\ \mathbf{C}_{21} & \mathbf{B} \end{pmatrix},$$

where $\mathbf{A} = [a_1, a_2]$ is a closed interval, \mathbf{B} , \mathbf{C}_{12} and \mathbf{C}_{21} are $s \times s$, $1 \times s$ and $s \times 1$ interval matrices, respectively. If

$$a_1 - \|\mathbf{C}_{12}\| L > m \sqrt{1 + L^2}$$

then for any $p \in (Q(p^) \cap B) \setminus \{p^*\}$ we have (17).*

4.3. Establishing heteroclinic connections. In this Section we combine the results of Sections 4.1, 4.2 to obtain a heteroclinic orbit between two fixed points of a map $f : \mathbb{R}^n \rightarrow \mathbb{R}^n$ in the special case that one of the fixed points is attracting. The existence of the attracting fixed point is established using the tools from Section 4.1. The other fixed point is hyperbolic, and has a one dimensional unstable manifold, as in Section 4.2. The next theorem is used to establish homoclinic connections between such two points. Computer assisted methods of proof for more general configurations are discussed in [48, 49, 50, 51].

Theorem 4.6. *Let $f : \mathbb{R}^n \rightarrow \mathbb{R}^n$ be C^1 and $B^1, B^2 \subset \mathbb{R}^n$ be two sets which are cartesian products of closed intervals in \mathbb{R}^n . Assume that the set B^1 satisfies the assumptions of Lemma 4.2. (that is, the assumptions hold for $B = B^1$.)*

Assume also that $p_2^ \in B^2 = B_u \times B_s$ is a hyperbolic fixed point and that the assumptions of Lemma 4.4 are satisfied.*

1. *If there exists an $n \geq 0$ and $\bar{x} \in B_u$ such that $f^n(Q(p_2^*) \cap \{p : \pi_u p = \bar{x}\}) \subset B^1$, then there exists an attracting fixed point $p_1^* \in B^1$ and a homoclinic orbit from p_1^* to p_2^* .*
2. *If there exists an $n \geq 0$, an interval $I \subset B_u$, and an $\bar{x} \in I$ such that $\pi_u f(Q(p_2^*) \cap \{p : \pi_u p = \bar{x}\}) \subset I$ and $f^n(\{p \in Q(p_2^*) : \pi_u p \in I\}) \subset B^1$, then there exists a C^0 curve, invariant under f , which joins p_1^* and p_2^* .*

Proof. We start by proving the first claim. We have $B_u \times B_s = B^2$ and by Lemma 4.4 there exists the function $w^u : B_u \rightarrow B^2$ which parameterizes the unstable manifold of p_2^* . Since w^u is a horizontal disc, it has the properties that $\pi_u w^u(x) = x$ and

that for any $x \in B_u$, $w^u(B_u) \subset Q(w^u(x))$; in particular $w^u(B_u) \subset Q(p_2^*)$. This means that $w^u(\bar{x}) \in Q(p_2^*) \cap \{p : \pi_u p = \bar{x}\}$. This by the assumption of our lemma implies that

$$f^n(w^u(\bar{x})) \subset f^n(Q(p_2^*) \cap \{p : \pi_u p = \bar{x}\}) \subset B^1.$$

By Lemma 4.2 the point p_1^* is attracting in B^1 , which means that

$$\lim_{k \rightarrow +\infty} f^k(w^u(\bar{x})) = p_1^*.$$

Since w^u parameterizes the unstable manifold of p_2^* we also have

$$\lim_{k \rightarrow -\infty} f^k(w^u(\bar{x})) = p_2^*,$$

which concludes the proof of the first claim.

To prove the second claim observe that $w^u(\bar{x}) \in Q(p_2^*) \cap \{p : \pi_u p = \bar{x}\}$, so

$$\pi_u f(w^u(\bar{x})) \subset \pi_u f(Q(p_2^*) \cap \{p : \pi_u p = \bar{x}\}) \subset I.$$

Let $x_1 := \bar{x}$ and $x_2 := \pi_u f(w^u(\bar{x}))$. The curve $w^u([x_1, x_2])$ is a fragment of the unstable manifold, which joins the point $w^u(\bar{x})$ with the point $f(w^u(\bar{x}))$. This means that for any $N \in \mathbb{N}$ we can define a continuous curve

$$\gamma_N := w^u(B_u) \cup \bigcup_{k=1}^N f^k(w^u([x_1, x_2])),$$

which coincides with a fragment of the unstable manifold. (The larger the N the larger the fragment). From our assumption

$$f^n(w^u([x_1, x_2])) \subset f^n(\{p \in Q(p_2^*) : \pi_u p \in I\}) \subset B^1.$$

Since f is contracting on B^1 , $f^k(w^u([x_1, x_2]))$ converge to p_1^* as k tends to infinity. This means that

$$\gamma := \bigcup_{N=1}^{\infty} \gamma_N \cup \{p_1^*\}$$

is a continuous curve joining p_1^* and p_2^* , as required. \square

5. Attracting invariant tori of ODEs in \mathbb{R}^3 . Consider a C^l , $l \geq 1$ vector field $F : \mathbb{R}^3 \rightarrow \mathbb{R}^3$. We are interested in the dynamics of the ODE

$$x' = F(x). \tag{18}$$

Our goal is to establish two types of invariant tori for the flow of (18). First, an attracting torus which is either C^k smooth, with $k \leq l$, or Lipschitz. The second is a torus that results from homoclinic connections of stable/unstable manifolds of periodic orbits.

Both types of tori are established by considering a section $\Sigma \subset \mathbb{R}^3$ and a section to section map $P : \Sigma \rightarrow \Sigma$ induced by the flow of the ODE. The first type of torus follows from the construction of invariant curves by taking $f = P$ and using the tools from Section 3. The second type follows from homoclinic connections between m -periodic orbits of P , which are established by taking $f = P^m$ and using the methods of Section 4.

The following theorem ensures that the invariant circle established using tools from Section 3 leads to an invariant Lipschitz torus. Let Φ_t denote the flow induced by (18).

Theorem 5.1. *Assume that $h^* : \mathbb{S}^1 \rightarrow \Sigma$ is a closed invariant curve (invariant for $f = P$). Let*

$$\mathcal{T} := \{ \Phi_t(v) : v \in h^*(\mathbb{S}^1), t \in \mathbb{R} \}.$$

1. *If h^* satisfies cone conditions (in the sense of Definition 3.3) then \mathcal{T} is a (two dimensional) Lipschitz invariant torus for (18).*
2. *If h^* is C^k then \mathcal{T} is a C^k invariant torus for (18).*

Proof. The set \mathcal{T} is a torus by construction. So we need to show that it is Lipschitz in the sense of Definition 2.3.

Take $p = \Phi_t(v) \in \mathcal{T}$. Assume that $v \in U_i$, meaning that $v \in \Sigma$ is in the local coordinates given by γ_i on Σ . (Throughout the reminder of the proof the p, v and t shall remain fixed.) We extend γ_i to a neighborhood of p by defining

$$\tilde{\gamma}_i(x_1, x_2, x_3) := \Phi_{t+x_2}(\gamma_i(a_i x_1, x_3)).$$

(Note that in $\tilde{\gamma}_i$ we have added a rescaling on the coordinate x_1 . The a_i used for the rescaling are the parameters from the cones Q_i in (2).) Take a small ball B around $\tilde{\gamma}_i^{-1}(p)$ and define $U := \tilde{\gamma}_i(B)$ and

$$\gamma_U := \tilde{\gamma}_i|_B.$$

Above U and γ_U are those needed for Definition 2.3.

We need that

$$U \cap \mathcal{T} \subset \gamma_U(\mathbf{Q}(\gamma_U^{-1}(\bar{q}_1)) \cap B).$$

This is equivalent to the condition that for any $q_1, q_2 \in U \cap \mathcal{T}$

$$\|\pi_{x_1, x_2}(\gamma_U^{-1}(q_1) - \gamma_U^{-1}(q_2))\| \geq \|\pi_{x_3}(\gamma_U^{-1}(q_1) - \gamma_U^{-1}(q_2))\|, \quad (19)$$

which is what we show below.

Before proving (19) we make the following auxiliary observation. Consider first $\bar{q}_1, \bar{q}_2 \in \mathcal{T} \cap \Sigma$. (Here we do not need \bar{q}_1, \bar{q}_2 to be in U . In fact, if p is far from Σ such \bar{q}_1, \bar{q}_2 will not be in U .) Since $\bar{q}_1, \bar{q}_2 \in h^*(\mathbb{S}^1)$ from the fact that h^* satisfies cone conditions it follows that $q_2 \notin \tilde{Q}_i(q_1)$ hence

$$\bar{q}_2 \notin \tilde{Q}_i(q_1) = \gamma_i(Q_i(\gamma_i^{-1}(\bar{q}_1))) = \tilde{\gamma}_i(\mathbf{Q}(\tilde{\gamma}_i^{-1}(\bar{q}_1))) \cap \Sigma = \gamma_U(\mathbf{Q}(\gamma_U^{-1}(\bar{q}_1))) \cap \Sigma. \quad (20)$$

Since $\bar{q}_1, \bar{q}_2 \in \Sigma$

$$\pi_{x_2} \tilde{\gamma}_i^{-1}(\bar{q}_1) = \pi_{x_2} \tilde{\gamma}_i^{-1}(\bar{q}_2) = -t,$$

so (20) implies

$$\|\pi_{x_1, x_2}(\gamma_U^{-1}(\bar{q}_1) - \gamma_U^{-1}(\bar{q}_2))\| \geq \|\pi_{x_3}(\gamma_U^{-1}(\bar{q}_1) - \gamma_U^{-1}(\bar{q}_2))\|. \quad (21)$$

Then we are ready to show (19). Take $q_1, q_2 \in U \cap \mathcal{T}$ where $q_1 = \Phi_{t_1}(\bar{q}_1)$, $q_2 = \Phi_{t_2}(\bar{q}_2)$ for $\bar{q}_1, \bar{q}_2 \in \mathcal{T} \cap \Sigma$ and some $t_1, t_2 \in \mathbb{R}$. By (21) we obtain

$$\begin{aligned} \|\pi_{x_1, x_2}(\gamma_U^{-1}(q_1) - \gamma_U^{-1}(q_2))\| &\geq \|\pi_{x_1}(\gamma_U^{-1}(q_1) - \gamma_U^{-1}(q_2))\| \\ &= \|\pi_{x_1}(\gamma_U^{-1}(\bar{q}_1) - \gamma_U^{-1}(\bar{q}_2))\| \\ &= \|\pi_{x_1, x_2}(\gamma_U^{-1}(\bar{q}_1) - \gamma_U^{-1}(\bar{q}_2))\| \\ &\geq \|\pi_{x_3}(\gamma_U^{-1}(\bar{q}_1) - \gamma_U^{-1}(\bar{q}_2))\| \\ &= \|\pi_{x_3}(\gamma_U^{-1}(q_1) - \gamma_U^{-1}(q_2))\|, \end{aligned}$$

as required.

The second claim follows directly from the fact that $(t, x) \rightarrow \Phi_t(x)$ is C^k . \square

The next result ensures that a homoclinic connection established using the tools from Section 4 gives an invariant torus for the ODE.

Lemma 5.2. *Assume that p_1^* is a point on a contracting k -periodic orbit of the Poincare map P and p_2^* is a point on a hyperbolic k -periodic orbit of P . If there exists a curve γ , invariant under P^k (i.e. $P^k(\gamma) = \gamma$), which joins p_1^* with p_2^* , such that $\bigcup_{i=1}^k P^i(\gamma)$ is a closed curve, then*

$$\mathcal{T} := \{\Phi_t(v) : v \in \gamma, t \in \mathbb{R}\}$$

is a two dimensional torus invariant under the flow of (18).

Proof. Continuing the curve $\bigcup_{i=1}^k P^i(\gamma)$ along the flow gives a two dimensional torus, as required. \square

6. Applications. In this Section we apply our methods to two explicit examples. The first is the Van der Pol system with periodic external forcing, where we prove the existence of smooth Lipschitz tori by means of the tools from Section 3. The second example is an autonomous vector field introduced by Langford [17] which exhibits a Neimark-Sacker bifurcation. For this system we establish the existence of C^0 tori by means of the tools from Section 4. An interesting aspect of the second example is that the tori are neither differentiable nor Lipschitz, so that C^0 is in fact the most that can be established. In all our computer assisted proofs we have used the CAPD² library.

6.1. Regular tori for the time dependent Van der Pol system. In this Section we apply the methods from Sections 3, 5 to establish the existence of C^k and Lipschitz tori in a periodically forced nonlinear oscillator. For our example application we consider the Van der Pol equation with periodic forcing

$$x'' - v(1 - x^2)x' + x - \varepsilon \cos(t) = 0.$$

The system is a canonical example in dynamical systems theory going back to its introduction by Balthasar van der Pol in 1920 as a mathematical model for an electrical circuit containing a vacuum tube [52]. For almost a century the system has been studied as a simple and physically relevant example of a differential equation exhibiting spontaneous nonlinear oscillations. Later van der Pol himself considered the circuit when driven by a periodic external forcing [53], and saw what would today be called an attracting invariant torus. For a much more complete theoretical discussion of the dynamics of the forced Van der Pol system, as well as a thorough review of the literature, we refer to the classic study of [54]. The interested reader is referred also to the works of [55, 56] for interesting applications of the forced system.

We prove the existence of a smooth and attracting invariant torus for the following pairs of parameters

$$(v, \varepsilon) \in \{(0.1, 0.002), (0.2, 0.005), (0.3, 0.01), (0.4, 0.015), (0.5, 0.05), (1, 0.1)\}. \quad (22)$$

To do so we consider the system in the extended phase space

$$\begin{aligned} x' &= y, \\ y' &= v(1 - x^2)y - x + \varepsilon \cos(t), \\ t' &= 1, \end{aligned} \quad (23)$$

²Computer Assisted Proofs in Dynamics: <http://capd.ii.uj.edu.pl/>

and take the time section $\Sigma = \{t = 0\}$. We consider the time shift map $f^{v,\varepsilon} : \Sigma \rightarrow \Sigma$ defined as $f^{v,\varepsilon}(x, y) = \Phi_{2\pi}^{v,\varepsilon}(x, y, 0)$, where $\Phi_s^{v,\varepsilon}$ is the flow induced by (23).

For each pair (v, ε) of parameters we take a sequence of points $\{p_i^{v,\varepsilon}\}_{i=1}^{N^{v,\varepsilon}} \subset \Sigma$, which lie approximately on the intersection of the torus with Σ . We draw these points in Figure 7. (These points are computed numerically. We choose them so that they are roughly uniformly spread along the curves.)

We then choose local coordinates $\gamma_i^{v,\varepsilon} : [-R_i^{v,\varepsilon}, R_i^{v,\varepsilon}] \times [-r^{v,\varepsilon}, r^{v,\varepsilon}] \rightarrow \mathbb{R}^2$ as

$$\gamma_i^{v,\varepsilon}(x, y) = q_i^{v,\varepsilon} + A_i^{v,\varepsilon} \begin{pmatrix} x \\ y \end{pmatrix} \quad \text{for } i = 1, \dots, N^{v,\varepsilon},$$

with

$$\begin{aligned} q_1^{v,\varepsilon} &= \frac{1}{2} (p_2^{v,\varepsilon} + p_N^{v,\varepsilon}), \\ q_N^{v,\varepsilon} &= \frac{1}{2} (p_1^{v,\varepsilon} + p_{N-1}^{v,\varepsilon}), \\ q_i^{v,\varepsilon} &= \frac{1}{2} (p_{i+1}^{v,\varepsilon} + p_{i-1}^{v,\varepsilon}), \quad \text{for } i = 2, \dots, N^{v,\varepsilon} - 1, \\ A_1^{v,\varepsilon} &= \frac{1}{R_1^{v,\varepsilon}} \begin{pmatrix} \pi_x \frac{1}{2} (p_2^{v,\varepsilon} - p_N^{v,\varepsilon}) & -\pi_y \frac{1}{2} (p_2^{v,\varepsilon} - p_N^{v,\varepsilon}) \\ \pi_y \frac{1}{2} (p_2^{v,\varepsilon} - p_N^{v,\varepsilon}) & \pi_x \frac{1}{2} (p_2^{v,\varepsilon} - p_N^{v,\varepsilon}) \end{pmatrix}, \\ A_N^{v,\varepsilon} &= \frac{1}{R_N^{v,\varepsilon}} \begin{pmatrix} \pi_x \frac{1}{2} (p_1^{v,\varepsilon} - p_{N-1}^{v,\varepsilon}) & -\pi_y \frac{1}{2} (p_1^{v,\varepsilon} - p_{N-1}^{v,\varepsilon}) \\ \pi_y \frac{1}{2} (p_1^{v,\varepsilon} - p_{N-1}^{v,\varepsilon}) & \pi_x \frac{1}{2} (p_1^{v,\varepsilon} - p_{N-1}^{v,\varepsilon}) \end{pmatrix}, \\ A_i^{v,\varepsilon} &= \frac{1}{R_i^{v,\varepsilon}} \begin{pmatrix} \pi_x \frac{1}{2} (p_{i+1}^{v,\varepsilon} - p_{i-1}^{v,\varepsilon}) & -\pi_y \frac{1}{2} (p_{i+1}^{v,\varepsilon} - p_{i-1}^{v,\varepsilon}) \\ \pi_y \frac{1}{2} (p_{i+1}^{v,\varepsilon} - p_{i-1}^{v,\varepsilon}) & \pi_x \frac{1}{2} (p_{i+1}^{v,\varepsilon} - p_{i-1}^{v,\varepsilon}) \end{pmatrix}, \end{aligned}$$

for $i = 2, \dots, N^{v,\varepsilon} - 1$, and

$$\begin{aligned} R_1^{v,\varepsilon} &= \left\| \frac{1}{2} (p_2^{v,\varepsilon} - p_N^{v,\varepsilon}) \right\|, \\ R_N^{v,\varepsilon} &= \left\| \frac{1}{2} (p_1^{v,\varepsilon} - p_{N-1}^{v,\varepsilon}) \right\|, \\ R_i^{v,\varepsilon} &= \left\| \frac{1}{2} (p_{i+1}^{v,\varepsilon} - p_{i-1}^{v,\varepsilon}) \right\|, \quad \text{for } i = 2, \dots, N^{v,\varepsilon} - 1. \end{aligned}$$

The choice is motivated by the fact that the set $\gamma_i([-R_i^{v,\varepsilon}, R_i^{v,\varepsilon}] \times \{0\})$ is a line connecting the points $p_{i-1}^{v,\varepsilon}$ and $p_{i+1}^{v,\varepsilon}$. As a result we obtain overlapping sets $U_i^{v,\varepsilon} := \gamma_i([-R_i^{v,\varepsilon}, R_i^{v,\varepsilon}] \times [-r^{v,\varepsilon}, r^{v,\varepsilon}])$ which cover the true invariant curve for $f^{v,\varepsilon}$. We establish the existence of the curve using the method outlined in Section 3.4. We outline some of the aspects of our computer assisted proof below.

For the first five parameters from (22) it turned out to be enough to consider $N^{v,\varepsilon} = 1000$. For these five parameters we have chosen $r^{v,\varepsilon} = 5 \cdot 10^{-4}$, and we have chosen the slope of the cones (2) as $a_i = 0.3$. Each set U_i was additionally subdivided into $m = 6$ parts for the validation of condition (12). This condition was the most time consuming part of the proof. The computer assisted proof for each of the four tori took under a minute and a half on a single 3 GHz Intel i7 Core processor. (The parameters r_i, a_i and m were chosen by trial and error.)

The validation of (12) was based on (13) so as a byproduct from (14) we obtained bounds on the derivatives of the local maps, which allows us to compute the bounds μ, ξ needed for the rate conditions (see Definition 3.7). By using Theorem 3.8 we validate the C^k regularity for the torus at parameter pairs $(v, \varepsilon) =$

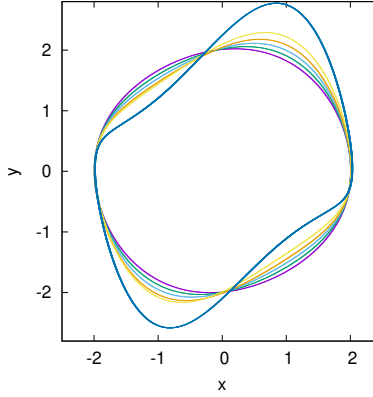


FIGURE 7. Intersections of the invariant Lipschitz tori for the Van der Pol system with the $t = 0$ section for each parameter from (22). The smaller the μ the more circular/smooth the curve.

$(0.1, 0.002)$, $(0.2, 0.005)$, $(0.3, 0.01)$ as $k = 9, 5, 2$, respectively. For the remaining parameters from (22) we only obtained that the tori are Lipschitz. This is due to the fact that the higher the v the less ‘uniform’ the dynamics on the torus. What we mean by this is that there are regions on the torus in which the dynamics restricted to the torus is expanding or contracting (the torus does not behave uniformly as a central coordinate). This affects the bounds on parameters μ, ξ (the second parameter in particular) which results in weaker regularity bounds obtained from our method.

Non-uniformity of the dynamics on the torus for higher v has also made the proof for the parameters $(v, \varepsilon) = (1, 0.1)$ more computationally demanding. We take $N^{v, \varepsilon} = 5000$ and $m = 20$, covering the curve with a larger number of fragments. We also take $r^{v, \varepsilon} = 2 \cdot 10^{-5}$, and the slope of the cones (2) were taken as $a_i = 0.1$. With a_i a larger number, but using smaller sets U_i allows us to validate the needed conditions in this example. The computer assisted proof for this parameter pair took 31 minutes on a single 3GHz Intel i7 Core processor.

This demonstrates the following weakness of our method. It performs well if the dynamics on the torus is uniform. If it is not, then proofs require many subdivisions. In the next Section we consider another example in which this problem is even more visible.

Remark 3. In the computer assisted proof we can use a small interval of parameters instead of a single parameter value. By invoking parallel computations on a cluster, one could use our approach to cover whole parameter ranges.

We finish with the comment that by Theorem 5.1 the invariant curves established for the map $f^{v, \varepsilon}$ lead to two dimensional invariant tori of (23).

6.2. Resonant tori in the Langford system. Consider the autonomous vector field $F : \mathbb{R}^3 \rightarrow \mathbb{R}^3$ given by the formula

$$F(x, y, z) = \begin{pmatrix} (z - \beta)x - \delta y \\ \delta x + (z - \beta)y \\ \gamma + \alpha z - \frac{z^3}{3} - (x^2 + y^2)(1 + \epsilon z) + \zeta z x^3 \end{pmatrix},$$

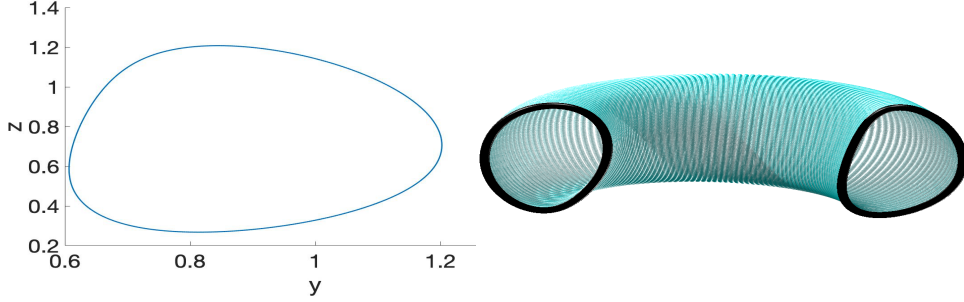


FIGURE 8. At $\alpha = 0.75$ we have an attracting limit cycle of P^2 on Σ (figure on the left) which is the intersection of the two dimensional C^k torus of the ODE with $\Sigma \cap \{y > 0\}$. On the right we plot half of the torus. In black we have both components of the torus intersection with Σ ; one for $y < 0$ and the other for $y > 0$.

where $\epsilon = 0.25$, $\gamma = 0.6$, $\delta = 3.5$, $\beta = 0.7$, $\zeta = 0.1$, and $\alpha = 0.95$ are the ‘classical’ parameter values. This system is a toy model for dissipative vortex dynamics, or for a rotating viscous fluid, and was first studied by Langford in [17]. We define a section $\Sigma = \{x = 0\}$, and the first return time section to section map $P : \Sigma \rightarrow \Sigma$.

We treat the parameter α as our bifurcation parameter. For all $\alpha \in [0, 0.95]$ there exists a fixed point in Σ of P^2 which corresponds to a periodic orbit τ of the ODE. The periodic orbit has complex conjugate Floquet multipliers which are stable for small α but which later cross the unit circle, losing stability in a Neimark-Sacker bifurcation [57], which occurs at $\alpha \approx 0.69714$ and gives birth to a C^k torus. We give a plot of such torus for one of the parameters in Figure 8.

Additionally there exist two period six orbits of P in Σ . One is a saddle periodic orbit which we denote as c_h , and the other is a stable focus periodic orbit, which we denote as c_s . (We use the subscript h to stand for ‘hyperbolic’ and s to stand for ‘stable’.) We found that one branch of $W^u(c_h)$ wraps around the torus, while the other reaches c_s ; see left plot in Figure 10. This happens right until $\alpha \approx 0.822$.

As we increase further our bifurcation parameter α , our invariant two-dimensional C^k torus bifurcates to a C^0 torus. This bifurcation happens by c_h, c_s colliding with the torus. Another way of interpreting this is by looking at what happens with $W^u(c_h)$ and $W^s(c_h)$. Before the bifurcation one branch of $W^u(c_h)$ goes inside, wrapping around the torus; see left plot from Figure 9. After the bifurcation both branches of $W^u(c_h)$ lead to c_s ; see right plot from Figure 9 and also Figure 11. Since after the bifurcation the tori include the periodic orbits, we refer to them as *resonant tori*.

For parameters between the case of C^k tori and the case of resonant tori we have transverse intersections of $W^u(c_h)$ and $W^s(c_h)$ as seen in Figure 10. This transverse intersection leads to the presence of Smale horseshoes and thus chaotic dynamics. These transverse intersections are born and terminated at parameters for which we have tangential intersections of $W^s(c_h)$ with $W^u(c_h)$.

Our objective is to apply the tools from Section 4.3 and prove the existence of a resonant tori. Below we describe the proof when $\alpha = 0.85$. The resonant torus in our proof is depicted in Figure 11.

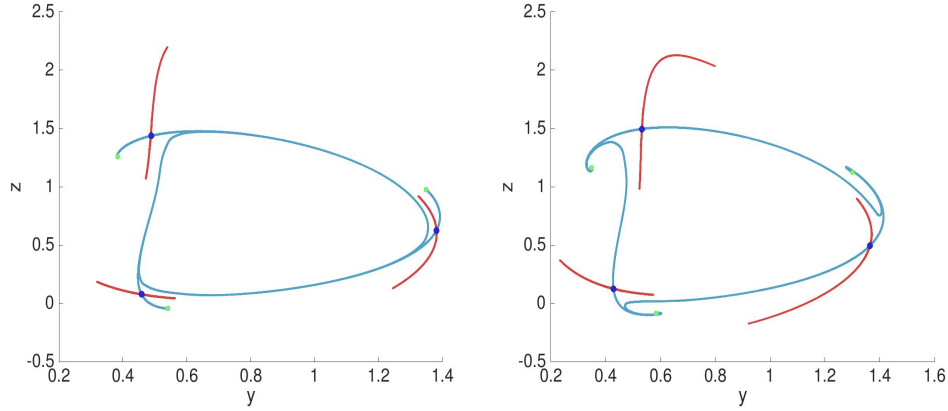


FIGURE 9. The plot of the periodic orbits c_h and c_s on $\Sigma \cap \{y > 0\}$. (The orbits are of period 6, but we plot only half of the points with $y > 0$.) The hyperbolic orbit c_u is in blue, and the attracting orbit c_s is in green. The manifold $W^s(c_h)$ is in red and $W^u(c_h)$ is blue. (Left) at $\alpha = 0.815$, we see that a branch of $W^u(c_h)$ goes inside and wraps around the attracting invariant circle. (Right) at $\alpha = 0.835$, we observe that a branch of $W^u(c_h)$ goes to the other side of $W^s(c_h)$ and gets caught in the basin of attraction of c_s .

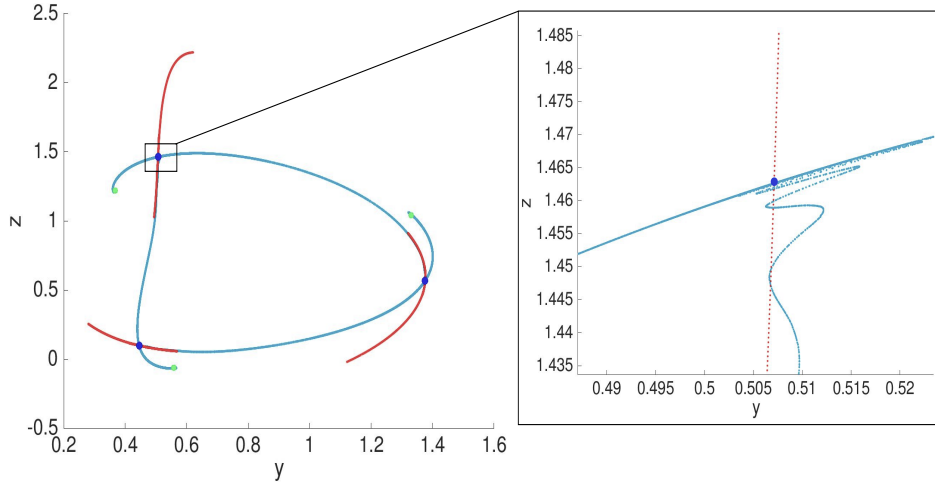


FIGURE 10. Colors have the same meaning as in Figure 9. At $\alpha = 0.8225$ we have transverse intersections of $W^u(c_h)$ and $W^s(c_h)$ which leads to chaotic dynamics.

Remark 4. We emphasize that the resonant torus from Figure 11 is continuous, but *not* C^k for $k > 0$. In fact, it is not even Lipschitz due to the rotation around the attractinmg periodic orbit.

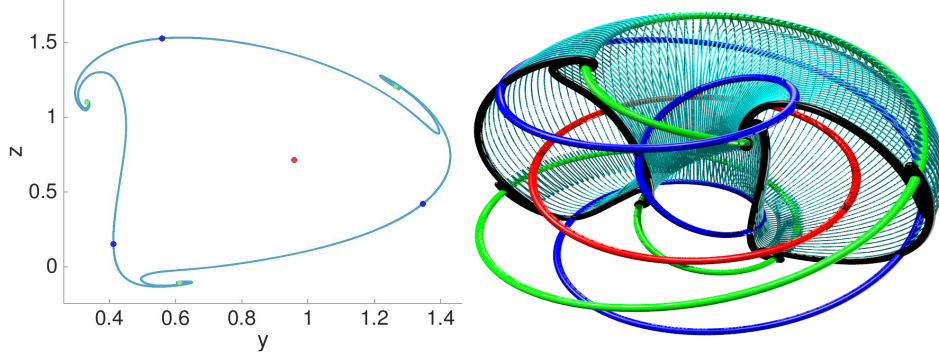


FIGURE 11. A resonance torus for $\alpha = 0.85$. In red we plot the periodic orbit from which the tori have initially originated through the Hopf type bifurcation.

We now outline the details of the proof. Consider the map $f : \mathbb{R}^2 \rightarrow \mathbb{R}^2$

$$f := P^6.$$

First we find bounds on two fixed points $p_1^*, p_2^* \in \Sigma$ of f , for which $p_1^* \in c_s$ and $p_2^* \in c_h$. We do this using the following shooting method. Consider

$$G : \underbrace{\mathbb{R}^2 \times \dots \times \mathbb{R}^2}_6 \rightarrow \mathbb{R}^{12},$$

defined as

$$G(q_1, \dots, q_6) := (P(q_6) - q_1, P(q_1) - q_2, P(q_2) - q_3, \dots, P(q_5) - q_6).$$

(Note that $q_i = (y_i, z_i) \in \Sigma$, for $i = 1, \dots, 6$.) Establishing that

$$G(q_1, \dots, q_6) = 0,$$

gives points q_1, \dots, q_6 on a period 6 orbit of P .

We using the interval Newton method (Theorem 2.2) to validate that the point (q_1, \dots, q_6) is in $\prod_{i=1}^{12} I_i$, for some closed intervals I_i , for $i = 1, \dots, 12$. Once this is done, the two dimensional box $I_1 \times I_2$ is an enclosure of q_1 which is a fixed point of P^6 . We find that

$$\begin{aligned} p_1^* &\in \begin{pmatrix} 0.611160359286522 + 4.6 \cdot 10^{-13} \cdot [-1, 1] \\ -0.104496536895459 + 8.8 \cdot 10^{-13} \cdot [-1, 1] \end{pmatrix}, \\ p_2^* &\in \begin{pmatrix} 0.413216691560642 + 2.5 \cdot 10^{-13} \cdot [-1, 1] \\ 0.150271844775546 + 9.4 \cdot 10^{-13} \cdot [-1, 1] \end{pmatrix}. \end{aligned}$$

Now take the two 2×2 matrices

$$\begin{aligned} A_1 &:= \begin{pmatrix} 0.953174 & -0.0468255 \\ 0.169128 & 0.2639 \end{pmatrix}, \\ A_2 &:= \begin{pmatrix} 0.0138304 & -1 \\ -1 & 0.674926 \end{pmatrix}, \end{aligned}$$

and define the local maps f_1 and f_2 around p_1^* and p_2^* , respectively, as

$$f_i(q) := A_i^{-1}(f(A_i q + p_i^*) - p_i^*) \quad \text{for } i = 1, 2.$$

Note that p_1^* and p_2^* are shifted to zero in their respective local coordinates. The choices of A_1 and A_2 are such that they put the derivatives of f_1 and f_2 , respectively, at zero approximately in Jordan form. Such A_1 and A_2 are computed using standard numerics (we do not need interval arithmetic validation at this stage).

We consider the two cubes B^1 and B^2 in \mathbb{R}^2 defined by

$$\begin{aligned} B^1 &:= [-0.0005, 0.0005] \times [-0.0005, 0.0005], \\ B^2 &:= [-0.0001, 0.0001] \times [-2 \cdot 10^{-8}, 2 \cdot 10^{-8}]. \end{aligned}$$

With computer assistance we established that zero is an attracting fixed point of f_1 in B^1 . This was done in interval arithmetic by using Lemma 4.2. We also established that the unstable manifold of zero for the map f_2 is contained in the cone $Q(0)$ of the form (15) with $L = 2 \cdot 10^{-4}$. We did this by using Lemma 4.4. The validation of the assumptions of Lemmas 4.2 and 4.4 was based on interval arithmetic bounds on the derivative of the map. Here we write out the bounds we have obtained:

$$\begin{aligned} [Df_1(B^1)] &= \begin{pmatrix} [0.150243, 0.220614] & [-0.561824, -0.521109] \\ [0.41934, 0.663593] & [0.10723, 0.263629] \end{pmatrix}, \\ [Df_2(B^2)] &= \begin{pmatrix} [2.16813, 2.16975] & [-0.000485, 0.000485] \\ [-0.000352, 0.000351] & [0.195584, 0.195806] \end{pmatrix}. \end{aligned}$$

We now consider

$$\bar{x} = 4.5 \cdot 10^{-5}.$$

With computer assistance we have validated that $\pi_u f_2(Q(0) \cap \{p : \pi_x p = \bar{x}\}) \subset I := [\bar{x}, 0.0001]$ and that for $n = 25$

$$A_1^{-1}(f^n(A_2(Q(0) \cap \{p : \pi_x p \in I\}) + p_2^*) - p_1^*) \subset B^1. \quad (24)$$

This by Theorem 4.6 establishes the existence of an invariant curve for f , which joins p_1^* and p_2^* . The resonant torus from Figure 11 follows from Lemma 5.2.

Remark 5. The condition (24) required $n = 25$ iterates of the map f , which is $6n = 150$ iterates of the map P ; this requires a long integration time of the ODE. This was the most time consuming part of the computer assisted proof, since it required a subdivision of $Q(0) \cap \{p : \pi_x p \in I\}$ into 200 fragments and checking (24) for each of them separately.

The computer assisted proof of the resonant torus for $\alpha = 0.85$ took under 6 minutes on a single 3GHz Intel i7 Core processor.

There is nothing particularly special about the parameter $\alpha = 0.85$. Using the same techniques, we have obtained proofs of resonant tori for other parameters, including $\alpha = 0.835$ for which we have the plot of the torus in the right hand plot from Figure 9.

We finish this Section by commenting on difficulties we have encountered when trying to validate the C^k tori for smaller parameters α . We ran into these when considering for instance $\alpha = 0.75$ for which the torus is plotted in Figure 8. Judging by the shape of the torus it would seem to be well suited for the validation methods of Section 3. Our problem in this particular example is that the dynamics near the torus are not uniformly contracting. There are some regions of expansion, and other regions of strong contraction. In total the torus is an attractor, but it is not a uniform one and the methods of Section 3 do not apply. When $\alpha = 0.75$ such uniform contraction is achieved for $f = P^{16}$. We have been able to enclose the curve in a set U which consists of 10000 cubes and validate that f is contracting in

U and that $f(U) \subset U$. (Such validation has been very time consuming and took 5 hours and 27 minutes on a single 3GHz Intel i7 Core processor.) This establishes the existence of an invariant set in U , but does not prove that this set is a torus. Using the results from [58] one obtains that this invariant set projects surjectively onto a torus, but other than this we do not get any information about its topology.

To prove that the invariant set is a torus we would need to also validate cone conditions. The fact that f consists of 16 iterates of P leads to long integration of the ODE. This resulted in insufficiently sharp estimates on the derivative of f and we were unable to validate cone conditions. An additional difficulty we have encountered is that in the neighborhood of the invariant curve of f we do not have ‘vertical’ contraction towards the curve, but also strong twist dynamics. This makes the validation of cone conditions even harder, since the angle between the center and the stable bundles becomes very small.

To be more precise, if on the section Σ we choose the tangent vector and the normal vector to the invariant circle as the basis for our coordinates, then for a point p from the invariant circle the derivative of $f = P^{16}$ is of the form

$$Df(p) = \begin{pmatrix} 1 & \delta \\ 0 & \lambda \end{pmatrix},$$

with $|\lambda| < 1$, but $|\lambda| \approx 1$, and $|\delta| \gg 1$. This means that in order to validate cone conditions, the fact that $(x, y) \in Q(0)$, i.e. $|y| < a|x|$, should imply that $Df(p)(x, y) \in Q(0)$, i.e. $|\lambda y| < a|x + y\delta|$. The choice of $y = -\delta^{-1}x$ will result in zero on the right hand side, which means that a necessary condition is to have $a \leq |\delta|^{-1}$. This means that in the case when δ is a large number (we have a strong twist), we have to choose small a , which means that we need to use sharp cones. The smaller the a the more difficult is the validation of cone conditions. On top of that, we need a large number of iterates of P to compute f , which leads to long integration times, resulting in insufficiently accurate bounds on the derivatives of f in order to validate the cone conditions.

We encounter exactly the same problem when the parameters of the system are close to the Neimark-Sacker bifurcation. In such setting the torus is not strongly attracting, meaning that a large number of iterates of P is needed for the contraction to be strong enough so that we can validate $f(U) \subset U$. This results in the appearance of a large twist parameter δ in derivatives of f , and we run into identical problems as those described above.

This demonstrates that our method has limitations in the presence of twist and nonuniform contraction of the invariant tori. Developing a computer assisted proof strategy which overcomes these difficulties would be an interesting future project. Another interesting project would be to formulate functional analytic methods for studying rotational invariant tori which could possibly lead to sharp or sharper regularity bounds.

7. Acknowledgements. We would like to thank the anonymous Reviewers for their comments, suggestions and corrections, which helped us improve our paper.

REFERENCES

- [1] Oscar E. Lanford, III. A computer-assisted proof of the Feigenbaum conjectures. *Bull. Amer. Math. Soc. (N.S.)*, 6(3):427–434, 1982.
- [2] Jean-Pierre Eckmann and Peter Wittwer. A complete proof of the Feigenbaum conjectures. *J. Statist. Phys.*, 46(3-4):455–475, 1987.

- [3] Warwick Tucker. The Lorenz attractor exists. *C. R. Acad. Sci. Paris Sér. I Math.*, 328(12):1197–1202, 1999.
- [4] Warwick Tucker. A rigorous ODE solver and Smale's 14th problem. *Found. Comput. Math.*, 2(1):53–117, 2002.
- [5] Jan Bouwe van den Berg and Jean-Philippe Lessard. Rigorous numerics in dynamics. *Notices Amer. Math. Soc.*, 62(9):1057–1061, 2015.
- [6] Javier Gómez-Serrano. Computer-assisted proofs in PDE: a survey. *SeMA J.*, 76(3):459–484, 2019.
- [7] Ju. I. Neimark. Some cases of the dependence of periodic motions on parameters. *Dokl. Akad. Nauk SSSR*, 129:736–739, 1959.
- [8] Robert John Sacker. *On Invariant Surfaces and Bifurcation of Periodic Solutions of Ordinary Differential Equations*. ProQuest LLC, Ann Arbor, MI, 1964. Thesis (Ph.D.)—New York University.
- [9] Seung-hwan Kim, R. S. MacKay, and J. Guckenheimer. Resonance regions for families of torus maps. *Nonlinearity*, 2(3):391–404, 1989.
- [10] C. Baesens, J. Guckenheimer, S. Kim, and R. S. MacKay. Three coupled oscillators: mode-locking, global bifurcations and toroidal chaos. *Phys. D*, 49(3):387–475, 1991.
- [11] Kunihiko Kaneko. Transition from torus to chaos accompanied by frequency lockings with symmetry breaking. In connection with the coupled-logistic map. *Progr. Theoret. Phys.*, 69(5):1427–1442, 1983.
- [12] Takashi Matsumoto, Leon O. Chua, and Ryuji Tokunaga. Chaos via torus breakdown. *IEEE Trans. Circuits and Systems*, 34(3):240–253, 1987.
- [13] O. Sosnovtseva and E. Mosekilde. Torus destruction and chaos-chaos intermittency in a commodity distribution chain. *Internat. J. Bifur. Chaos Appl. Sci. Engrg.*, 7(6):1225–1242, 1997.
- [14] Taoufik Bakri, Yuri A. Kuznetsov, and Ferdinand Verhulst. Torus bifurcations in a mechanical system. *J. Dynam. Differential Equations*, 27(3-4):371–403, 2015.
- [15] Taoufik Bakri and Ferdinand Verhulst. Bifurcations of quasi-periodic dynamics: torus breakdown. *Z. Angew. Math. Phys.*, 65(6):1053–1076, 2014.
- [16] Luca Dieci, Jens Lorenz, and Robert D. Russell. Numerical calculation of invariant tori. *SIAM J. Sci. Statist. Comput.*, 12(3):607–647, 1991.
- [17] W. F. Langford. Numerical studies of torus bifurcations. In *Numerical methods for bifurcation problems (Dortmund, 1983)*, volume 70 of *Internat. Schriftenreihe Numer. Math.*, pages 285–295. Birkhäuser, Basel, 1984.
- [18] Àlex Haro and Rafael de la Llave. A parameterization method for the computation of invariant tori and their whiskers in quasi-periodic maps: rigorous results. *J. Differential Equations*, 228(2):530–579, 2006.
- [19] Àlex Haro and Rafael de la Llave. A parameterization method for the computation of invariant tori and their whiskers in quasi-periodic maps: numerical algorithms. *Discrete Contin. Dyn. Syst. Ser. B*, 6(6):1261–1300, 2006.
- [20] Àlex Haro and Rafael de la Llave. A parameterization method for the computation of invariant tori and their whiskers in quasi-periodic maps: explorations and mechanisms for the breakdown of hyperbolicity. *SIAM J. Appl. Dyn. Syst.*, 6(1):142–207, 2007.
- [21] Marta Canadell and Àlex Haro. Computation of quasi-periodic normally hyperbolic invariant tori: algorithms, numerical explorations and mechanisms of breakdown. *J. Nonlinear Sci.*, 27(6):1829–1868, 2017.
- [22] Marta Canadell and Àlex Haro. Computation of quasiperiodic normally hyperbolic invariant tori: rigorous results. *J. Nonlinear Sci.*, 27(6):1869–1904, 2017.
- [23] Marta Canadell and Àlex Haro. Parameterization method for computing quasi-periodic reducible normally hyperbolic invariant tori. In *Advances in differential equations and applications*, volume 4 of *SEMA SIMAI Springer Ser.*, pages 85–94. Springer, Cham, 2014.
- [24] Neil Fenichel. Persistence and smoothness of invariant manifolds for flows. *Indiana Univ. Math. J.*, 21:193–226, 1971/72.
- [25] Morris W. Hirsch and Charles C. Pugh. Stable manifolds and hyperbolic sets. In *Global Analysis (Proc. Sympos. Pure Math., Vol. XIV, Berkeley, Calif., 1968)*, pages 133–163. Amer. Math. Soc., Providence, R.I., 1970.
- [26] M. W. Hirsch, C. C. Pugh, and M. Shub. Invariant manifolds. *Bull. Amer. Math. Soc.*, 76:1015–1019, 1970.

- [27] M. W. Hirsch, C. C. Pugh, and M. Shub. *Invariant manifolds*. Lecture Notes in Mathematics, Vol. 583. Springer-Verlag, Berlin-New York, 1977.
- [28] Carles Simó. Connection of invariant manifolds in the n -body problem, $n > 3$. In *Proceedings of the sixth conference of Portuguese and Spanish mathematicians, Part II (Santander, 1979)*, number 2, part 2, pages 1257–1261, 1979.
- [29] Jaume Llibre, Regina Martínez, and Carles Simó. Transversality of the invariant manifolds associated to the Lyapunov family of periodic orbits near L_2 in the restricted three-body problem. *J. Differential Equations*, 58(1):104–156, 1985.
- [30] H. W. Broer, H. M. Osinga, and G. Vegter. On the computation of normally hyperbolic invariant manifolds. In *Nonlinear dynamical systems and chaos (Groningen, 1995)*, volume 19 of *Progr. Nonlinear Differential Equations Appl.*, pages 423–447. Birkhäuser, Basel, 1996.
- [31] H. W. Broer, H. M. Osinga, and G. Vegter. Algorithms for computing normally hyperbolic invariant manifolds. *Z. Angew. Math. Phys.*, 48(3):480–524, 1997.
- [32] B. Krauskopf, H. M. Osinga, E. J. Doedel, M. E. Henderson, J. Guckenheimer, A. Vladimírsky, M. Dellnitz, and O. Junge. A survey of methods for computing (un)stable manifolds of vector fields. *Internat. J. Bifur. Chaos Appl. Sci. Engrg.*, 15(3):763–791, 2005.
- [33] Hinke M. Osinga. Computing global invariant manifolds: techniques and applications. In *Proceedings of the International Congress of Mathematicians—Seoul 2014. Vol. IV*, pages 1101–1123. Kyung Moon Sa, Seoul, 2014.
- [34] Alessandra Celletti and Luigi Chierchia. Rigorous estimates for a computer-assisted KAM theory. *J. Math. Phys.*, 28(9):2078–2086, 1987.
- [35] Alessandra Celletti and Luigi Chierchia. A computer-assisted approach to small-divisors problems arising in Hamiltonian mechanics. In *Computer aided proofs in analysis (Cincinnati, OH, 1989)*, volume 28 of *IMA Vol. Math. Appl.*, pages 43–51. Springer, New York, 1991.
- [36] Rafael de la Llave and David Rana. Accurate strategies for small divisor problems. *Bull. Amer. Math. Soc. (N.S.)*, 22(1):85–90, 1990.
- [37] Rafael de la Llave and David Rana. Accurate strategies for K.A.M. bounds and their implementation, computer aided proofs in analysis (cincinnati, oh, 1989). *IMA Vol. Math. Appl.*, 28:127–146, 1991.
- [38] J.-Ll. Figueras, À. Haro, and A. Luque. Rigorous computer-assisted application of KAM theory: a modern approach. *Found. Comput. Math.*, 17(5):1123–1193, 2017.
- [39] Àlex Haro and Alejandro Luque. A-posteriori KAM theory with optimal estimates for partially integrable systems. *J. Differential Equations*, 266(2-3):1605–1674, 2019.
- [40] Rafael de la Llave. Invariant manifolds associated to nonresonant spectral subspaces. *J. Statist. Phys.*, 87(1-2):211–249, 1997.
- [41] Daniel Wilczak and Piotr Zgliczyński. C^n Lohner algorithm. *Scheade Informaticae*, 20:9–46, 2011.
- [42] Piotr Zgliczyński. C^1 Lohner algorithm. *Found. Comput. Math.*, 2(4):429–465, 2002.
- [43] Maciej J. Capiński. Computer assisted existence proofs of Lyapunov orbits at L_2 and transversal intersections of invariant manifolds in the Jupiter-Sun PCR3BP. *SIAM J. Appl. Dyn. Syst.*, 11(4):1723–1753, 2012.
- [44] Piotr Zgliczyński. Covering relations, cone conditions and the stable manifold theorem. *J. Differential Equations*, 246(5):1774–1819, 2009.
- [45] G. Alefeld. Inclusion methods for systems of nonlinear equations—the interval Newton method and modifications. In *Topics in validated computations (Oldenburg, 1993)*, volume 5 of *Stud. Comput. Math.*, pages 7–26. North-Holland, Amsterdam, 1994.
- [46] Maciej J. Capiński and Piotr Zgliczyński. Cone conditions and covering relations for topologically normally hyperbolic invariant manifolds. *Discrete Contin. Dyn. Syst.*, 30(3):641–670, 2011.
- [47] Maciej J. Capiński and Piotr Zgliczyński. Geometric proof for normally hyperbolic invariant manifolds. *J. Differential Equations*, 259(11):6215–6286, 2015.
- [48] Daniel Wilczak, Sergio Serrano, and Roberto Barrio. Coexistence and dynamical connections between hyperchaos and chaos in the 4D Rössler system: a computer-assisted proof. *SIAM J. Appl. Dyn. Syst.*, 15(1):356–390, 2016.
- [49] Gianni Arioli and Hans Koch. Existence and stability of traveling pulse solutions of the FitzHugh-Nagumo equation. *Nonlinear Anal.*, 113:51–70, 2015.
- [50] J. D. Mireles James and Konstantin Mischaikow. Rigorous a posteriori computation of (un)stable manifolds and connecting orbits for analytic maps. *SIAM J. Appl. Dyn. Syst.*, 12(2):957–1006, 2013.

- [51] Jean-Philippe Lessard, Jason D. Mireles James, and Christian Reinhardt. Computer assisted proof of transverse saddle-to-saddle connecting orbits for first order vector fields. *J. Dynam. Differential Equations*, 26(2):267–313, 2014.
- [52] B. van der Pol. A theory of the amplitude of free and forced triode vibrations. *Radio Review*, 1:701–710, 754–762, 1920.
- [53] B. van der Pol. Frequency demultiplication. *Nature*, 120:363–364, 1927.
- [54] John Guckenheimer, Kathleen Hoffman, and Warren Weckesser. The forced van der Pol equation. I. The slow flow and its bifurcations. *SIAM J. Appl. Dyn. Syst.*, 2(1):1–35, 2003.
- [55] J.E. Flaherty and F.C. Hoppensteadt. Frequency entrainment of a forced van der pol oscillator. declassified Air Force report AD A 03921, 1997.
- [56] M. Cercek, Tomaz Gyergyek, and Mladen Stanojevic. On the nonlinear dynamics of an instability in front of a positively biased electrode in a magnetized plasma. Nuclear Energy in Central Europe, Portoroz, Slovenia, 16-19 September, pp. 531–538, 1996.
- [57] Emmanuel Fleurantin and Jason D. Mireles-James. Transport barriers, resonance tori, and torus-chaos in a vector field with a neimark-sacker bifurcation. arXiv:1905.08828.
- [58] Maciej J. Capiński and Hieronim Kubica. Persistence of normally hyperbolic invariant manifolds in the absence of rate conditions. arXiv:1804.05580.

Received xxxx 20xx; revised xxxx 20xx.

E-mail address: maciej.capinski@agh.edu.pl

E-mail address: efleurantin2013@fau.edu

E-mail address: jmirelesjames@fau.edu